# Comparative electromechanical and hemodynamic effects of left ventricular and biventricular pacing in dyssynchronous heart failure: *electrical resynchronization versus left-right ventricular interaction*

**Running Title:** Mechanism of pacing therapy in failing hearts

Joost Lumens, PhD,*† Sylvain Ploux, MD,*† Marc Strik, MD,† John Gorcsan III, MD,‡ Hubert Cochet, MD,* Nicolas Derval, MD,* Maria Strom, PhD,§ Charu Ramanathan, PhD,§ Philippe Ritter, MD,* Michel Haïssaguerre, MD,* Pierre Jaïs, MD,* Theo Arts, PhD,† Tammo Delhaas, MD, PhD,† Frits W. Prinzen, PhD,† Pierre Bordachar, MD, PhD*

*Hôpital Cardiologique du Haut-Lévêque, CHU Bordeaux, IHU LIRYC, Bordeaux, France; †Maastricht University Medical Center, Cardiovascular Research Institute Maastricht (CARIM), Maastricht, The Netherlands; ‡University of Pittsburgh, Pittsburgh, PA; §Cardioinsight Technologies, Cleveland, OH.

## Online Supplement A: protocol animal experiments

A 7F catheter tip manometer (CD-Leycom Zoetermeer, the Netherlands) was used for continuous RV pressure measurement. A second 7F catheter tip manometer combined with conductance catheter was used to measure LV pressure and volume. The pressure and volume data were used to quantify pacing-induced changes of LV and RV $dP/dt_{max}$, LV stroke volume, and LV pump stroke work (i.e., area of pressure-volume relation). In all dogs, a pacing lead was inserted transvenously into the right atrium, close to the entrance of the inferior caval vein. After thoracotomy, two multi-electrode arrays (total of 102 epicardial electrodes) were placed around the heart and a multi-electrode catheter (6 electrodes) on the RV-side of the septum to enable measurement of local LV and RV epicardial electrograms (1). Fluoroscopy was used to ensure a stable position of the latter multi-electrode catheter with its tip electrode in the RV apex and the remaining 5 sensing electrodes contacting the septal myocardium. Positioning was assumed successful when all 6 electrodes acquired stable full-cycle ECG signals. Two additional electrodes were used for LV apical and apicolateral mapping. The tip electrode of the RV multi-electrode catheter and an epicardial LV basolateral electrode were used for LVP and BiVP. All measurements were performed during right atrial pacing at approximately 10 bpm above intrinsic heart rate (baseline) and during atrial paced LVP and BiVP with the same heart rate and short AV delay ensuring full

ventricular capture as noticed on the surface ECG. Hemodynamic and electrocardiographic data were recorded for a minimum of two respiratory cycles. Each measurement was preceded by a baseline recording.

## Online Supplement B: model description

### *Model Design*

The CircAdapt model of the human heart and circulation is configured as a network composed of a limited number of module types representing myocardial walls, cardiac valves, large blood vessels, and peripheral vasculature (Figure S1A) (2,3). In each cardiac chamber, the CircAdapt model requires cavity pressure to be known as a function of cavity and wall volumes only. Large blood vessels (arteries and veins) are represented by non-linear elastic vessel modules having characteristic impedance for pressure-flow waves. Vessels and chambers are connected by valves, having inertia and Bernoulli pressure losses. Effective orifice area of a cardiac valve depends on direction and magnitude of flow through the valve and on pressure drop over the valve. Peripheral pulmonary and systemic vascular beds are modeled by non-linear resistances connecting the pulmonary and systemic arterial and venous vessel modules. The resulting pulmonary and systemic circulations allow hemodynamic interaction between the left and right side of the heart. Atria and ventricles are represented by chambers with a wall composed of contractile myocardial tissue, which is also handled as a module. Myocardial tissue is simulated by a non-linear elastic material, harboring myofibers that contract after depolarization (3). Vascular tissue is considered non-linearly elastic. Furthermore, the pericardium is modeled as a passive elastic sheet surrounding the entire heart (ventricles and atria) (4). Finally, the CircAdapt model generates traces of hemodynamic and mechanical variables (such as cardiac and vascular pressures and volumes, flow through cardiac valves, and local myofiber stress–strain relationship in the constituting walls) as a function of time and covering the entire cardiac cycle.

### *Ventricular mechanics (TriSeg module)*

The ventricular section of the CircAdapt model (TriSeg module) has previously been described in more detail (3). Briefly, three wall segments, representing the LV free wall (LVFW), the interventricular septum (SEPT), and the RV free wall (RVFW), meet at a common junction and thereby form both the LV and RV cavity. Mechanical ventricular interaction is incorporated by stating tensional force equilibrium at the junction. Global LV and RV pump mechanics (pressure–volume relation) are related to representative myofiber mechanics (stress–strain relation) in the three ventricular walls (Figure S1B), using the

principle of conservation of mechanical work. In each individual wall, the myofiber stress–strain relation is determined by a three-element Hill model that describes active and passive cardiac myofibre mechanics (3). The latter model of sarcomere mechanics incorporates experimental findings on isolated cardiac muscle (5,6), i.e., strength and duration of activation increase with sarcomere length, while velocity of sarcomere shortening increases with passive stretch.

***Global wall mechanics (Wall module)***

Given the geometry of each ventricular wall $i$ (in terms of mid-wall area $A_{m,i}$, mid-wall curvature $C_{m,i}$, and wall volume $V_{w,i}$), natural myofiber strain ($\varepsilon_{f,i}$) is calculated using

$$\varepsilon_{f,i} = \frac{1}{2}\ln\left(\frac{A_{m,i}}{A_{m,ref,i}}\right) - \frac{1}{12}z_i^2 - 0.019z_i^4 \qquad \text{with } z_i = \frac{3C_{m,i}V_{w,i}}{2A_{m,i}} \qquad \text{(Eq. 1)}$$

where $A_{m,ref,i}$ represents reference mid-wall area. Then, Cauchy myofiber stress ($\sigma_{f,i}$) is derived from $\varepsilon_{f,i}$ using a three-element Hill model that describes active and passive cardiac tissue mechanics (3).

$$\sigma_{f,i} = \text{function}(\varepsilon_{f,i}) \qquad \text{(Eq. 2)}$$

Representative mid-wall tension ($T_{m,i}$) is calculated from $\sigma_{f,i}$ and wall geometry using

$$T_{m,i} = \frac{V_{w,i}\sigma_{f,i}}{2A_{m,i}}\left(1 + \frac{z_i^2}{3} + \frac{z_i^4}{5}\right) \qquad \text{(Eq. 3)}$$

Finally, LV and RV pressures are derived from mid-wall tension and global geometry of the LV and RV free walls, respectively (3).

***Local wall mechanics (Patch module)***

Although the simplified representation of each ventricular wall by a single myofiber allows inhomogeneity of material properties between ventricular walls, it does not allow local inhomogeneities within a single wall. Therefore, the existing CircAdapt model is extended

with a module that enables subdivision of each cardiac wall into any desired number ($n$) of mechanically coupled patches, each having its own tissue properties (Figure S1B). For each ventricular wall $i$, total wall volume and mid-wall area equal the sum of these volumes of all patches:

$$V_{w,i} = \sum_{j=1}^{n} V_{w,i,j} \quad \text{(Eq. 4)}$$

$$A_{m,i} = \sum_{j=1}^{n} A_{m,i,j} \quad \text{(Eq. 5)}$$

Mid-wall curvature is common to all patches and depends on total midwall area:

$$C_{m,i,j} = C_{m,i}\left(A_{m,i}\right) \quad \text{(Eq. 6)}$$

Furthermore, in each patch, mid-wall tension depends on mid-wall area of the patch. Also mid-wall tension is the same in all patches of a ventricular wall, resulting in the set of equations:

$$T_{m,i,j}\left(A_{m,i,j}\right) = T_{m,i} \quad \text{(Eq. 7)}$$

Given total mid-wall area $A_{m,i}$, tension $T_{m,i}$ and patch areas $A_{m,i,j}$ are obtained by solving the set of equations as described by Eqs. 4 and 7.

***Local myofiber mechanics (Myofiber module)***

In each wall patch, the myocardial tissue has been modeled as previously described in more detail by Lumens *et al* (3). In brief, the myofiber is represented by a passive element in parallel with a series combination of a contractile element and series elastic element. The time dependent behavior is described by two state variables, i.e., contractile element length ($L_{sarc,i,j}$) and mechanical activation ($C_{sarc,i,j}$). The latter activation parameter is physiologically related to intracellular calcium concentration. The time derivative of $L_{sarc,i,j}$ depends linearly on length of the series elastic element and equals zero for isometric contraction, while the time derivative of $C_{sarc,i,j}$ depends on time ($t$), $L_{sarc,i,j}$, and $C_{sarc,i,j}$.

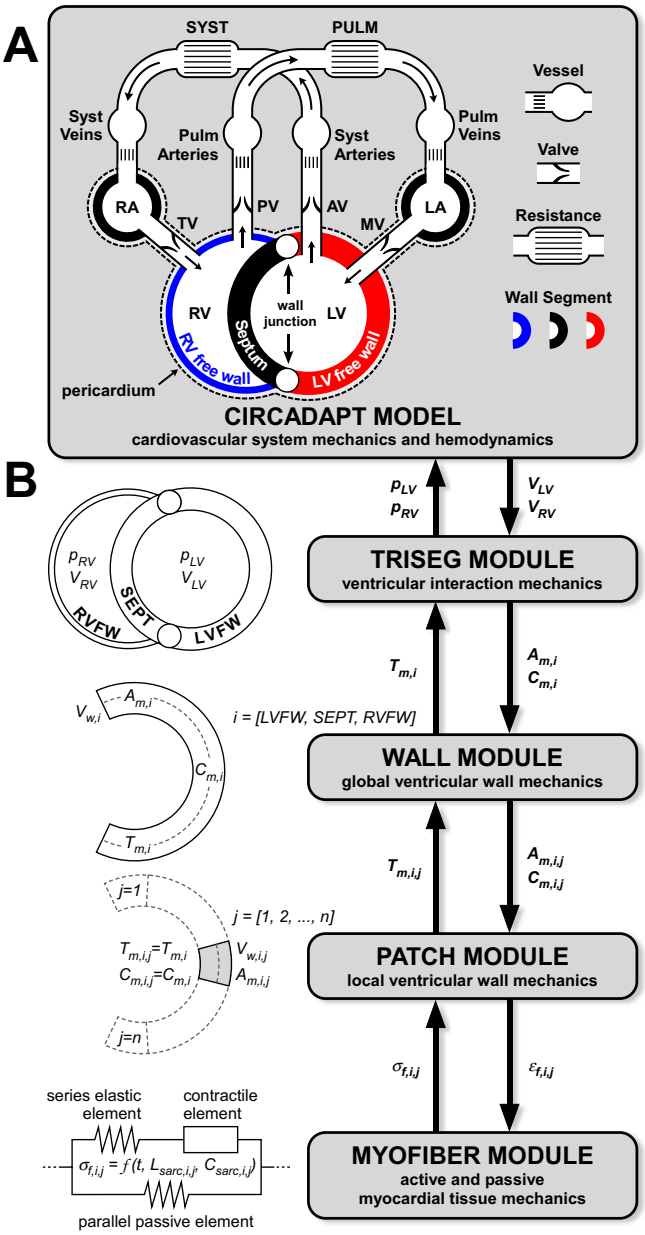


***Figure S1:*** *Design of the CircAdapt model of the heart and circulation.* ***A)*** *The closed-loop circulation is configured as a network of modules representing cardiac walls (atrial and ventricular), blood vessels (arteries and veins), cardiac valves (AV=aortic valve; MV=mitral valve; PV=pulmonary valve; TV=tricuspid valve), and peripheral vasculature (PULM=pulmonary; SYST=systemic).* ***B)*** *The flow of calculations in the ventricular module (3) of the CircAdapt model. Starting from LV and RV cavity volumes ($V_{LV}$ and $V_{RV}$, respectively), ventricular pressures ($p_{LV}$ and $p_{RV}$) are calculated by 1) relating ventricular mechanics (pressure as function of volume) to wall mechanics (tension as function of wall area and curvature), 2) relating global wall mechanics to local wall mechanics, and 3)*

*relating local wall mechanics to local myofiber mechanics (myofiber stress as function of myofiber strain).*

**Online Supplement C: simulation protocol**

Mechanics and hemodynamics of the normal cardiovascular system with nonfailing myocardium and synchronous activation of the ventricular walls were simulated as published previously (4,7). Starting from this normal condition, a failing heart with LBBB was simulated in four steps:

- the ventricular myocardium was subdivided in 23 segments (11 LV free wall, 5 septum, and 7 RV free wall) of equal mass (9 g per segment). Onset time of activation of each ventricular segment was adjusted so that a typical LBBB-sequence of ventricular activation with an $AT_{TOT}$ of 135 ms was obtained (Figure S2);
- the AV delay was set to 220 ms, being close to the average PR-interval measured in the patients;
- a state of global myocardial contractile failure was obtained by reducing myofiber contractility of all ventricular segments to 40% of its normal value so that LV ejection fraction equaled 23%; and
- heart rate was set to 80 bpm and systemic peripheral resistance and total circulating blood volume were adjusted so that mean arterial pressure and cardiac output were 92 mmHg and 4.2 l/min, respectively.

Using the resulting simulation as the baseline reference situation, LVP and BiVP were simulated by changing the sequence of ventricular activation as depicted in Figure S2 and by shortening the AV delay to 100 ms. Pacing was assumed to lead to full ventricular capture. These acute changes of local ventricular activation and AV delay were chosen so that they were in agreement with the electrocardiographic mapping data obtained in the patients and dogs, i.e., LVP did not change $AT_{TOT}$ (135 ms), whereas BiVP was assumed to reduce $AT_{TOT}$ to 60 ms.

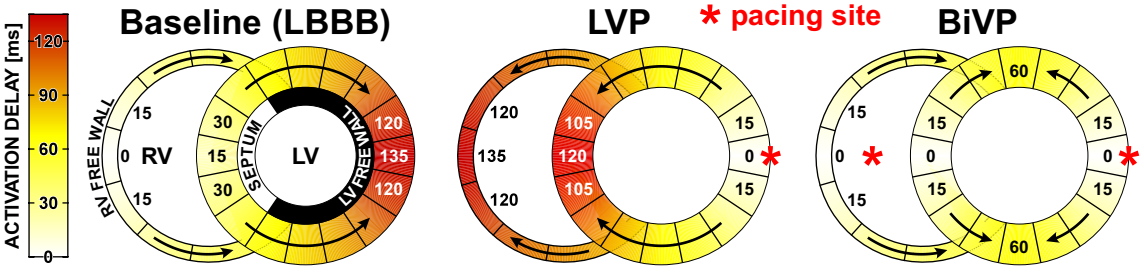


***Figure S2:*** *Local delays of onset ventricular activation during baseline (LBBB), LVP, and BiVP. Pacing sites are indicated by red asterisks.*

**REFERENCES**


1. Strik M, Rademakers LM, van Deursen CJ et al. Endocardial left ventricular pacing improves cardiac resynchronization therapy in chronic asynchronous infarction and heart failure models. Circ Arrhythm Electrophysiol 2012;5:191-200.
2. Arts T, Delhaas T, Bovendeerd P, Verbeek X, Prinzen FW. Adaptation to mechanical load determines shape and properties of heart and circulation: the CircAdapt model. Am J Physiol Heart Circ Physiol 2005;288:H1943-54.
3. Lumens J, Delhaas T, Kirn B, Arts T. Three-Wall Segment (TriSeg) Model Describing Mechanics and Hemodynamics of Ventricular Interaction. Ann Biomed Eng 2009;37:2234-2255.
4. Leenders GE, Lumens J, Cramer MJ et al. Septal deformation patterns delineate mechanical dyssynchrony and regional differences in contractility: analysis of patient data using a computer model. Circ Heart Fail 2012;5:87-96.
5. de Tombe PP, ter Keurs HE. Force and velocity of sarcomere shortening in trabeculae from rat heart. Effects of temperature. Circ Res 1990;66:1239-54.
6. ter Keurs HE, Rijnsburger WH, van Heuningen R, Nagelsmit MJ. Tension development and sarcomere length in rat cardiac trabeculae. Evidence of length-dependent activation. Circ Res 1980;46:703-14.
7. Lumens J, Leenders GE, Cramer MJ et al. Mechanistic Evaluation of Echocardiographic Dyssynchrony Indices: Patient Data Combined with Multiscale Computer Simulations. Circ Cardiovasc Imaging 2012;5:491-499.

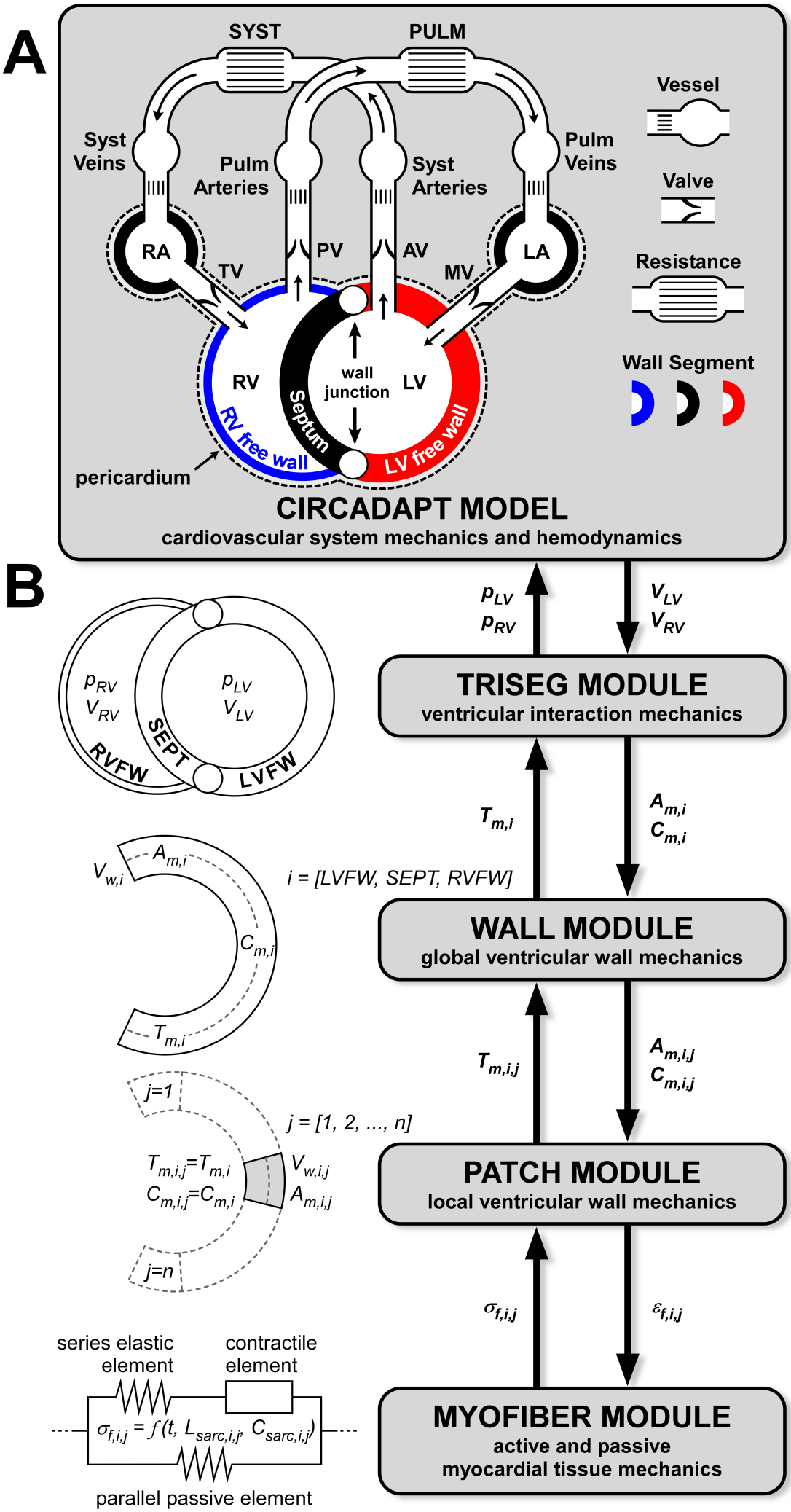
A
SYST
PULM
Syst Veins
Pulm Arteries
Syst Arteries
Pulm Veins
RA
TV
PV
AV
MV
LA
RV
wall junction
LV
Septum
RV free wall
LV free wall
pericardium
Vessel
Valve
Resistance
Wall Segment
CIRCADAPT MODEL
cardiovascular system mechanics and hemodynamics
B
$p_{RV}$ $V_{RV}$
$p_{LV}$ $V_{LV}$
RVFW
SEPT
LVFW
$p_{LV}$ $p_{RV}$
$V_{LV}$ $V_{RV}$
TRISEG MODULE
ventricular interaction mechanics
$T_{m,i}$
$A_{m,i}$ $C_{m,i}$
$V_{w,i}$
$A_{m,i}$
$C_{m,i}$
$T_{m,i}$
i = [LVFW, SEPT, RVFW]
WALL MODULE
global ventricular wall mechanics
$T_{m,i,j}$
$A_{m,i,j}$ $C_{m,i,j}$
j=1
j=n
$T_{m,i,j}=T_{m,i}$
$C_{m,i,j}=C_{m,i}$
$V_{w,i,j}$
$A_{m,i,j}$
j = [1, 2, ..., n]
PATCH MODULE
local ventricular wall mechanics
$\sigma_{f,i,j}$
$\varepsilon_{f,i,j}$
series elastic element
contractile element
$\sigma_{f,i,j} = f(t, L_{sarc,i,j}, C_{sarc,i,j})$
parallel passive element
MYOFIBER MODULE
active and passive
myocardial tissue mechanics

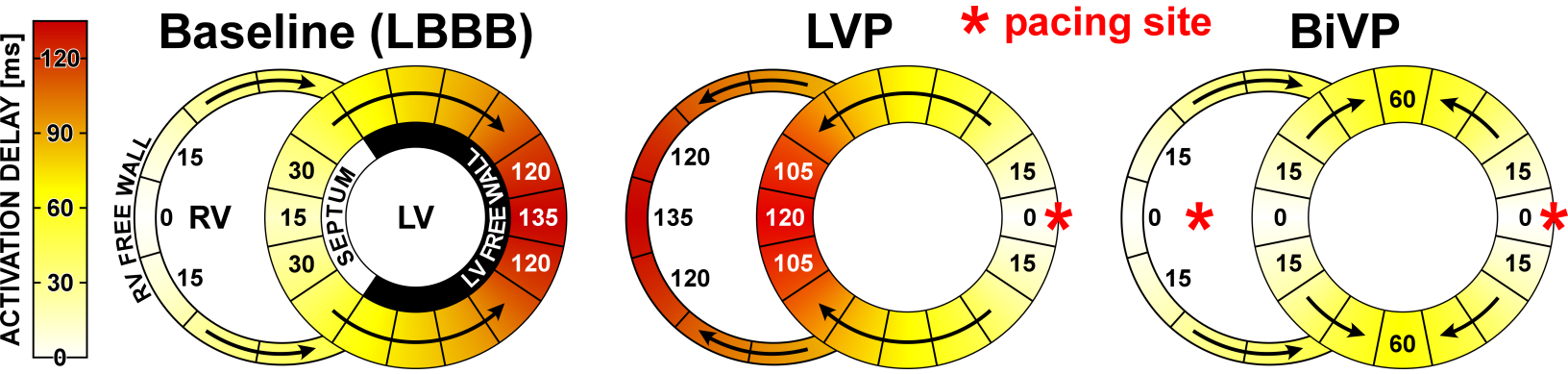
ACTIVATION DELAY [ms]
120
90
60
30
0
Baseline (LBBB)
RV FREE WALL
15
0
RV
15
30
15
30
SEPTUM
LV
LV FREE WALL
120
135
120
LVP
* pacing site
120
135
120
105
120
105
15
0
15
BiVP
15
0
15
15
0
15
60
15
0
15
60